ACS APPLIED MATERIALS & INTERFACES

Research Article

www.acsami.org

Sensitive Water Probing through Nonlinear Photon Upconversion of Lanthanide-Doped Nanoparticles

Shaohong Guo,[†] Xiaoji Xie,*[,†] Ling Huang,*[,†] and Wei Huang*[,†,‡]

[†]Key Laboratory of Flexible Electronics (KLOFE), Institute of Advanced Materials (IAM), Jiangsu National Synergetic Innovation Center for Advanced Materials (SICAM), Nanjing Tech University (NanjingTech), Nanjing 211816, China

[‡]Key Laboratory for Organic Electronics and Information Displays, Institute of Advanced Materials, Jiangsu National Synergetic Innovation Center for Advanced Materials (SICAM), Nanjing University of Posts & Telecommunications, Nanjing 210023, China

Supporting Information

ABSTRACT: Lanthanide-doped upconversion nanoparticles have received growing attention in the development of low-background, highly sensitive and selective sensors. Here, we report a water probe based on ligand-free $NaYF_4$:Yb/Er nanoparticles, utilizing their intrinsically nonlinear upconversion process. The water molecule sensing was realized by monitoring the upconversion emission quenching, which is mainly attributed to efficient energy transfer between upconversion nanoparticles and water molecules as well as water-absorption-induced excitation energy attenuation. The nonlinear upconversion process, together with power function relationship between upconversion emission intensity and excitation power density, offers a sensitive detection of water content down to 0.008 vol % (80 ppm) in an organic solvent. As an added benefit, we show that noncontact detection of water can be achieved just by using water attenuation effect. Moreover, these upconversion nanoparticle based recyclable probes should be particularly suitable for real-time and long-term water monitoring, due to their superior chemical and physical stability. These results could provide insights into the design of upconversion nanoparticle based sensors.

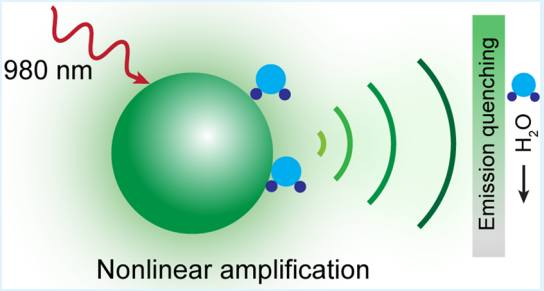

KEYWORDS: *upconversion, lanthanide-doped nanoparticles, luminescence, sensor, water*

INTRODUCTION

Water, the major constituent of the fluids of living things, is vital for all known forms of life. However, the transparent liquid sometimes is regarded as contaminant and could be destructive, even in a small amount, when it exists in many products, such as fuels, organic solvents, electronics, and pharmaceuticals.[1−3] The measurement of water, therefore, is of great interest not only for fundamental research but also for many promises in technological applications. Till now, a variety of optical sensors have been developed to probe water, including fluorescent/luminescent sensors,[1−10] optical fiber sensors,[11] and waveguide sensors,[12] as alternatives to the standard Karl Fischer method.[13] Indeed, the optical water sensors offer several advantages over traditional analysis methods, such as simple operation, fast response, and reliable optical readout. For example, organic luminescent molecule based sensors have been proven effective for water detection with a high sensitivity, down to ppm level, in organic phase.[6] Despite the advances, the majority of the organic molecule based sensors suffer from poor reusability.[3,4,6] Moreover, these sensors are typically not suitable for in situ or long-term water content monitoring because of their weak photostability upon ultraviolet light excitation.

Lanthanide-doped upconversion nanoparticles recently have received considerable attention due to their unique properties, including large anti-Stokes shift, sharp fingerprint emission, and high photostability.[14−20] Particularly, benefiting from the near-infrared light excitation, upconversion nanomaterials enable bioimaging and biosensing with deep penetration depth and low background interference.[21−27] Typically, upconversion nanoparticle based sensors rely on the upconversion luminescence energy transfer to probe analytes. In these cases, the luminescent changes of upconversion nanoparticles allow analyte sensing with unsurpassed sensitivity. By utilization of this principle, sensors, targeting metal ions, biomolecules, and small molecules have been developed.[28−31]

Developing upconversion nanoparticles with strong emission and high upconversion efficiency is crucial for the sensing platforms to afford outstanding performance. However, upconversion nanoparticles typically suffer from luminescence quenching caused by energy interplay between the nanoparticles and surrounding molecules, particularly water molecules.[32,33] Several methods, for example, inert-shell passivation, have been developed to minimize the surface quenching effect.[34−48] Meanwhile, such quenching effect opens up a new opportunity for probing water molecules by using lanthanide-doped upconversion nanoparticles. Considering the nonlinear upconversion process as well as power function relationship between upconversion emission intensity and

Received: October 24, 2015
Accepted: December 11, 2015
Published: December 11, 2015

DOI: 10.1021/acsami.5b10192
ACS Appl. Mater. Interfaces 2016, 8, 847−853

excitation power density, we reason that sensitive detection of water can be realized using upconversion nanoparticles.

In our design, we select hexagonal $NaYF_4$ hosted upconversion nanoparticles as nanoprobes, owing to its low phonon energy and capability to generate intense upconversion emissions.[49] Water molecules in dispersion can accept the energy from excited lanthanide ions and attenuate the excitation energy by direct light absorption (Figure 1). The

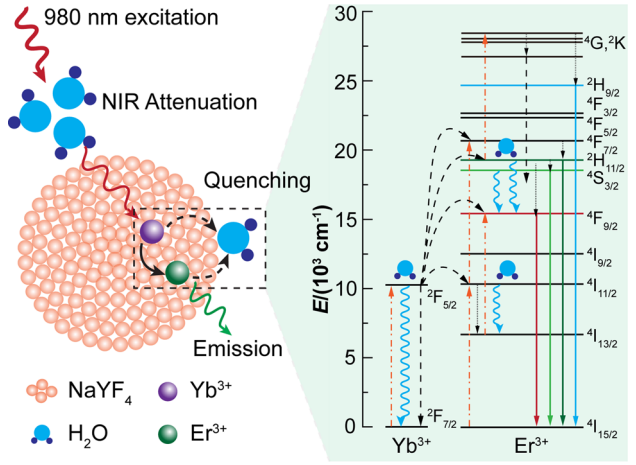

Figure 1. Schematic illustration of water molecule induced upconversion emission quenching of $NaYF_4$:Yb/Er nanoparticles. Water molecules can absorb part of the excitation energy before excitation light reaches nanoparticles. Upon excitation of the nanoparticle, Yb^{3+} and Er^{3+} ions, in their excitation states, can transfer their energy to the nearby water molecules. Consequently, the upconversion emission is suppressed. Energy level diagrams on the right panel illustrate the proposed upconversion mechanisms. The dashed-dotted, dashed, dotted, wavy, and solid arrows represent photon excitation, energy transfer, multiphonon relaxation, water induced energy depletion, and emission process, respectively.

efficient excitation energy depletion would result in a rapid and remarkable decrease in the luminescence of upconversion nanoparticles and thus reveals the existence of water molecules. On the basis of this design, we successfully detect water in a wide range of concentrations from ~0.01 to 100 vol % in organic solvents, such as *N*,*N*-dimethylformamide (DMF), dimethyl sulfoxide (DMSO), and ethanol. The detection limit can be down to 80 ppm in DMF. As an added benefit, the upconversion nanoparticle probes can be recollected and reused without obvious changes in their sensing behavior. In addition, a noncontact method for water detection has also been demonstrated by utilizing water molecule caused excitation power attenuation. These results imply the feasibility of using upconversion nanoparticles, as recyclable luminescent probes, for sensitive detection of water based on nonlinear upconversion amplification. The findings presented here can also provide new insight into the development of other optical sensors by leveraging nonlinear upconversion process of lanthanide-doped nanoparticles.

EXPERIMENTAL SECTION

Materials. Yttrium(III) acetate hydrate (99.9%), ytterbium(III) acetate hydrate (99.9%), erbium(III) acetate hydrate (99.9%), oleic acid (90%) were purchased from Alfa Aesar. 1-Octadecene (90%) was purchased from Sigma-Aldrich. Sodium hydroxide (NaOH, >98%), ammonium fluoride (NH_4F, >98%), and all other chemicals were purchased from Sinopharm Chemical Reagent Beijing Co., Ltd. All chemicals were used as received unless otherwise noted.

Synthesis of $NaYF_4$:Yb/Er Core Nanoparticles and $NaYF_4$:Yb/Er@$NaYF_4$ Core–Shell Nanoparticles. $NaYF_4$:Yb/Er core nanoparticles and $NaYF_4$:Yb/Er@$NaYF_4$ core–shell nanoparticles were prepared according to a literature procedure.[42] A 2 mL aqueous solution containing $Y(CH_3CO_2)_3$ (0.1082 g, 0.32 mmol), $Yb(CH_3CO_2)_3$ (0.0252 g, 0.072 mmol), and $Er(CH_3CO_2)_3$ (0.0033 g, 0.008 mmol) was mixed with 3 mL of oleic acid and 7 mL of 1-Octadecene in a 50 mL two-neck round-bottom flask. The resulting mixture was stirred at 150 °C for 60 min to remove water before cooling down to 50 °C. Subsequently, a methanol solution (6 mL) of NaOH (0.04 g, 1 mmol) and NH_4F (0.0593 g, 1.6 mmol) was added and stirred at 50 °C for 30 min, followed by heating at 100 °C for another 30 min. After purging with nitrogen, the reaction mixture was heated to 290 °C and kept for 1.5 h before cooling down to room temperature. The resulting nanoparticles were collected by centrifugation at 6000 rpm for 5 min and washed with ethanol three times. The $NaYF_4$:Yb/Er core nanoparticles were finally dispersed in cyclohexane (4 mL) for further use.

The preparation of $NaYF_4$:Yb/Er@$NaYF_4$ core–shell nanoparticles used the $NaYF_4$:Yb/Er core nanoparticles as seeds for further shell coating. Typically, the shell stock solution was prepared by mixing a 2 mL aqueous solution of $Y(CH_3CO_2)_3$ (0.1352 g, 0.4 mmol), 3 mL of oleic acid, and 7 mL of 1-Octadecene in a 50 mL flask. The mixture was then stirred at 150 °C for 60 min before cooling down to 50 °C. A cyclohexane dispersion (4 mL) of $NaYF_4$:Yb/Er core nanoparticles was added along with a methanol solution (6 mL) of NaOH (0.04 g, 1 mmol) and NH_4F (0.0593 g, 1.6 mmol). The reaction mixture was then stirred at 50 °C for 30 min and 100 °C for 30 min before nitrogen purging. Subsequently, the solution was heated to 290 °C and kept for 1.5 h before cooling down to room temperature. The resulting core–shell nanoparticles were collected by centrifugation and washed with ethanol several times before being dispersed in cyclohexane.

Synthesis of Ligand-Free Nanoparticles. Ligand-free upconversion nanoparticles were obtained according to a literature procedure with slight modification.[50] The oleic acid coated nanoparticles were dispersed in a mixture of ethanol (1 mL) and hydrochloric acid (1 mL, 2 M) and then ultrasonicated for 2 min to remove the oleic acid. The ligand-free nanoparticles were collected by centrifugation at 16 500 rpm for 15 min, washed with ethanol three times, and redispersed in water.

Water Detection in Organic Solvent. The ligand-free upconversion nanoparticles, along with varied amounts of water, were first added into an organic solvent (e.g., DMF, DMSO, and ethanol) to afford testing solutions with an identical concentration of upconversion nanoparticles (0.1 mg/mL). The upconversion emission profiles of the resulting dispersions were then recorded, in a sealed quartz cuvette, from 400 to 700 nm under the excitation of a 980 nm diode laser.

Measurements. Transmission electron microscopy (TEM) measurements were obtained on a Hitachi 7700 transmission electron microscope at an acceleration voltage of 100 kV. High resolution TEM (HRTEM) images and energy-dispersive X-ray (EDX) spectra were carried out on a Tecnai G2 F20 microscope. Powder X-ray diffraction (XRD) data were recorded on a Rigaku Smartlab (9 kW) X-ray diffractometer with Cu Kα radiation (λ = 1.5406 Å). Fourier transform infrared (FTIR) spectra were obtained from a Nicolet (iS10) FTIR spectrometer. The UV–visible–near-infrared spectra were measured on a PerkinElmer (Lambda35) spectrometer. Upconversion fluorescence spectra were recorded on a fluorescent spectrometer (Hitachi F-4600 FL) equipped with a power adjustable diode laser (980 nm). The luminescent decay curves were recorded on an Edinburgh FSP920 spectrometer equipped with a photomultiplier (PMT), in conjunction with either a modulated 980 nm diode laser or a nanosecond optical parametric oscillator (OPO) pumped by a 3.8 ns pulsed Nd:YAG laser (Ekspla, NT352) as the excitation source. All the measurements were performed at room temperature unless otherwise noted.

DOI: 10.1021/acsami.5b10192
ACS Appl. Mater. Interfaces 2016, 8, 847–853

RESULTS AND DISCUSSION

Preparation and Characterization of Ligand-Free Upconversion Nanoparticles. To examine the possibility of using upconversion nanoparticles for water molecule probing, we first synthesized hexagonal phase $NaYF_4$:Yb/Er (18/2 mol %) nanoparticles through well-developed thermal coprecipitation method. The as-prepared $NaYF_4$:Yb/Er (18/2 mol %) nanoparticles, capped by oleic acid, have high uniformity in size (average size of ~22 nm) and morphology (Figure S1). Powder X-ray diffraction pattern confirms a pure hexagonal phase of $NaYF_4$ of the obtained $NaYF_4$:Yb/Er nanoparticles (Figure S2).

We then removed the surface ligand, oleic acid, by hydrochloride acid treatment to make ligand-free nanoparticles. Fourier transform infrared spectrum (FTIR) of the ligand-free nanoparticles, without characteristic peaks of oleic acid, confirms the removal of surface ligand (Figure S3). The ligand-free nanoparticles remain in their morphology after acid treatment (Figure 2a), with an average size of ~21 nm (Figure 2b). It should be noted that the slight size change could be attributed to the hydrochloride acid etching of $NaYF_4$. Nevertheless, the ligand-free nanoparticles retain hexagonal phase and single-crystalline nature, as indicated by the high-resolution transmission electron microscopy and powder X-ray diffraction (Figure S4). Energy-dispersive X-ray (EDX) spectrum confirms the presence of Na^+, Y^{3+}, F^-, and Yb^{3+} in ligand-free nanoparticles (Figure S4).

We next studied the luminescence properties of the ligand-free $NaYF_4$:Yb/Er nanoparticles under excitation of 980 nm diode laser at room temperature. As expected, typical emission bands of Er^{3+}, located at ~540 and ~655 nm, which were attributed to the transitions from $^4S_{3/2}$, $^2H_{11/2}$, and $^4F_{9/2}$ to $^4I_{15/2}$, were observed (Figure 2c). The ligand-free nanoparticles, in water, give a larger ratio of red-to-green emission when compared to that of the oleic acid capped nanoparticles dispersed in cyclohexane. This could be attributed to the changes of surface ligand and solvent.

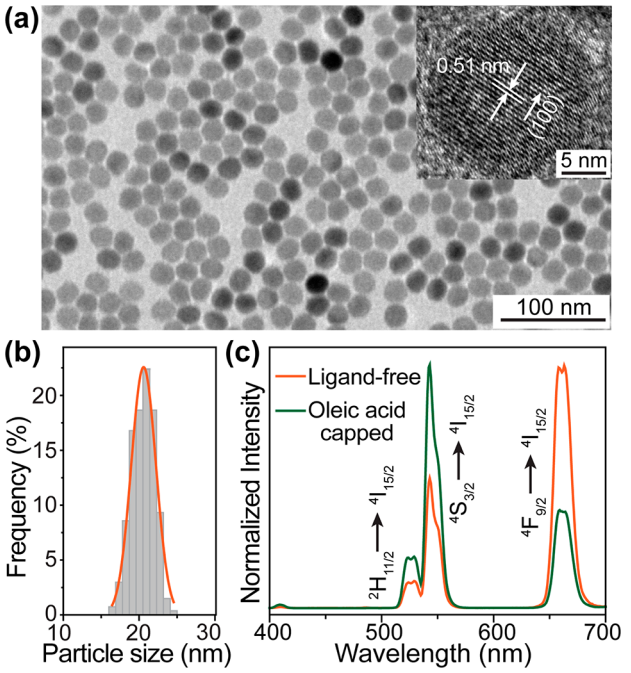

Figure 2. (a) Low resolution TEM image of the ligand-free $NaYF_4$:Yb/Er (18/2 mol %) nanoparticles. Inset: High resolution TEM image of a single ligand-free nanoparticle. (b) Corresponding size distribution of ligand-free nanoparticles in (a). (c) Room-temperature upconversion emission spectra of the oleic acid capped $NaYF_4$:Yb/Er (18/2 mol %) nanoparticles dispersed in cyclohexane and the corresponding ligand-free nanoparticles dispersed in H_2O, respectively. All spectra were obtained under 980 nm laser excitation, and the concentration of nanoparticles was ~1 mg/mL.

Water Detection in Organic Solvent. To prove water sensing in organic solvent, we first chose DMF as a representative and prepared a series of testing solutions containing ligand-free nanoparticles and different amounts of water. Upon exciting these DMF solutions by a 980 nm laser, we found that the upconversion emission was gradually quenched with the increase of water in the solution (Figure 3a). In contrast, the intensity ratio of red-to-green emission increases while water concentration rises (Figure S5). Intriguingly, neither the upconversion emission intensity nor the red-to-green ratio is linearly related to the water content, which is different from the observation of typical luminescence energy transfer based upconversion sensors. Within the water concentration range of 0.008–100 vol %, we found that the integrated emission intensity exhibits two-separated linearity with logarithm of water concentration (vol %) (Figure 3b), which indicates a nonlinear quenching effect. Notably, the linear correlation coefficient of each calibration curve is larger than 0.99, and the detection of water in DMF can be down to

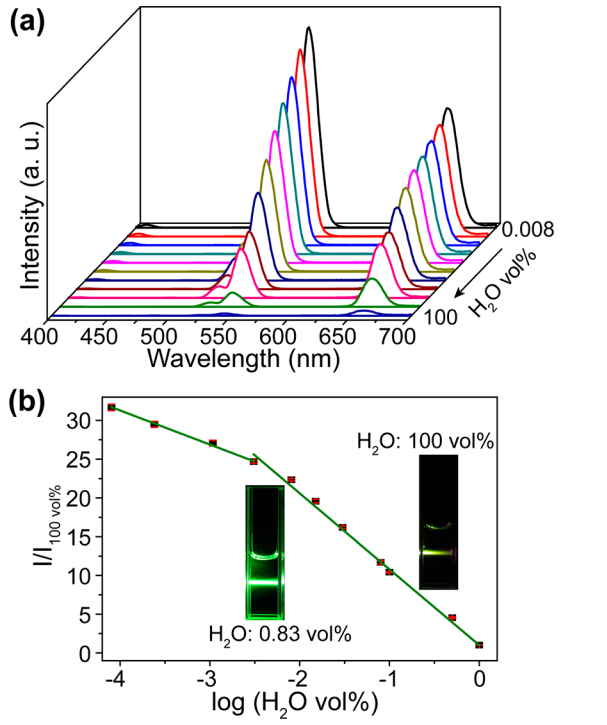

Figure 3. (a) Upconversion emission changes of ligand-free $NaYF_4$:Yb/Er nanoparticles as a function of H_2O concentration (0.008–100 vol %) in DMF. (b) Corresponding relative emission intensity ($I/I_{100\ vol\%}$) dependence on H_2O concentration. The insets are the luminescence photographs of nanoparticles, excited by 980 nm laser, in DMF containing 0.83 vol % of H_2O and pure water, respectively. Note that the emission intensity was obtained by integrating the emission from 400 to 700 nm. Data are presented as the average from three measurements.

DOI: 10.1021/acsami.5b10192
ACS Appl. Mater. Interfaces 2016, 8, 847–853

0.008% (80 ppm) according to the calibration curve. Moreover, the nanoparticles are reusable for water sensing. To demonstrate the reusability of these nanoparticles, ligand-free nanoparticles were collected after water sensing, dried in oven, and then redispersed. Utilizing these redispersed nanoparticles, we can get similar luminescence response to water molecules in DMF (Figure S6).

In the following set of experiments, we checked the photostability of ligand-free upconversion nanoparticles and the upconversion luminescence response to the addition of water. We first monitored the upconversion emission, in a testing solution (H_2O/DMF, 10/90 vol %), up to 25 min under the excitation of 980 nm laser. The luminescence signal quickly became stable and remained almost identical even after 25 min of continuous laser excitation (Figure S7). To demonstrate the possibility of in situ water monitoring, we continuously recorded the upconversion emission profiles upon water addition to a DMF testing solution. A steady response was quickly achieved within 2 min as indicated by the stable step curve (Figure 4). Next, we introduced various organic dyes as

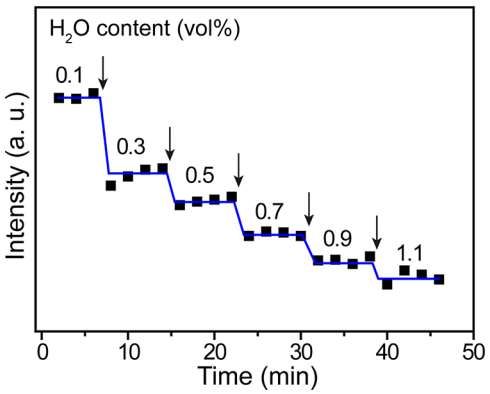

Figure 4. Upconversion emission response to five-time additions of H_2O to a DMF testing solution over 40 min, under continuous 980 nm laser excitation. The solid arrows indicate the addition of water. Note that the emission intensity was obtained by integrating the emission from 400 to 700 nm. The blue line serves as a guide to the eye.

disruptors to check the response of these nanoparticle probes. Benefiting from the near-infrared excitation and upconversion process, no obvious interference was observed when the testing solution contained disruptors, such as fluorene, carbazole, and pyrene (Figure S8). Notably, owing to the intrinsic fluorescence emission, the presence of organic dyes could largely affect the performance of typical fluorescence sensors which are excited by ultraviolet light. These results reveal that the ligand-free upconversion nanoparticles are suitable for long-term, real-time, and in situ monitoring of water content, even in complex samples.

To demonstrate the versatility of the method, we studied the performance of ligand-free $NaYF_4$:Yb/Er nanoparticles in other organic solvents, like DMSO and ethanol, for water sensing. Similar to the case in DMF, a sequential luminescence quenching was observed with the increase of water in both DMSO and ethanol (Figures S9 and S10). Meanwhile, the integrated emission intensity exhibits different relationship with logarithm of water concentration (vol %) when compared with that in DMF. These observations imply that organic solvent molecules may have interplay with both ligand-free nanoparticles and water molecules, which affect the upconversion emission. For example, -OH group of ethanol can also extract excitation energy from excited lanthanide ions. In addition, C–H bond vibrations of solvent molecules can participate in the depletion of excitation energy. These factors should account for the difference in the water sensing performance while using different organic solvents. Together, these results indicate that ligand-free upconversion nanoparticles can be used as efficient probes for water molecule detection in various samples, such as organic solvent and deuterated solvent.

Energy Transfer between Upconversion Nanoparticles and Water Molecules. To elucidate the water quenching effect, we measured the luminescent lifetime of ligand-free $NaYF_4$:Yb/Er nanoparticles dispersed in a series of DMF solutions. We first studied lifetimes of Er^{3+} emission centered at 540 and 654 nm. As illustrated in Figures 5a, 5b, S11 and Table S1, the lifetimes of green and red emission were reduced with the increase of water content, indicating a strong nonradiative energy transfer from Er^{3+} ions to water molecules. During the energy transfer process, $^4S_{3/2}$ and $^2H_{11/2}$ states, responsible for the green emission, can be depopulated to red emitting $^4F_{9/2}$ state and thus give rise to an increase in the intensity ratio of the red-to-green emission (Figure S5). The lifetime of Yb^{3+} ions was then recorded under the excitation of 975 nm laser, and a remarkable lifetime decrease was observed (Figures 5c, S11 and Table S2). Compared with the lifetimes of Er^{3+}, the lifetime of Yb^{3+} is more sensitive to water molecules, which could be ascribed to the good match between the energy of $^2F_{5/2}$ state and vibration energy of -OH group.

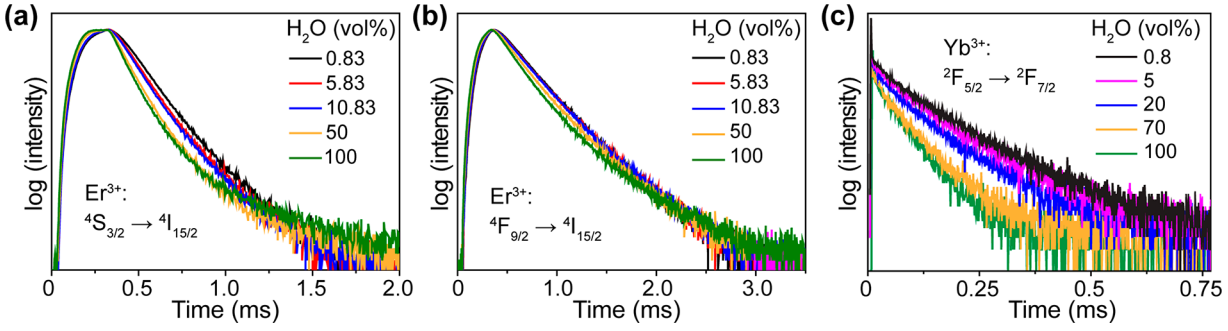

Figure 5. Upconversion luminescence decay curves of ligand-free $NaYF_4$:Yb/Er nanoparticles dispersed in DMF containing varied water content. (a, b) Decay curves of Er^{3+} measured at 540 and 654 nm (excitation: 980 nm), respectively. The water concentration was 0.83, 5.83, 10.83, 50, and 100 vol %, respectively. (c) Decay curves of Yb^{3+} measured at 985 nm (excitation: 975 nm). The water concentration was 0.8, 5, 20, 70, and 100 vol %, respectively.

DOI: 10.1021/acsami.5b10192
ACS Appl. Mater. Interfaces 2016, 8, 847–853

Notably, the energy transfer, from excited Er^{3+} and Yb^{3+} to water molecules, is not restricted to those ions located on the surface of nanoparticle. To prove this, we coated $NaYF_4$:Yb/Er nanoparticles with an inert $NaYF_4$ shell. After removal of the surface ligand, the thickness of $NaYF_4$ shell was ~2.3 nm (Figure S12). Emission lifetimes of the resulting ligand-free core−shell nanoparticles, in DMF solution with varied water content, were recorded (Figure S14). Generally, the luminescent lifetimes of core−shell nanoparticles are prolonged when compared to those of core nanoparticles under the same conditions. Despite the prolonged lifetimes, a sharp decrease of lifetimes was also observed with the increase of water content. The results indicate that a thin layer of $NaYF_4$ shell cannot efficiently prevent the excitation energy transfer from upconversion nanoparticles to water molecules. These findings also imply the energy transfer, like Yb^{3+}-to-Yb^{3+} energy migration, from the inner core to the particle surface may contribute to the sensitive detection of water. In fact, by using the ligand-free core−shell nanoparticles, we can also realize water sensing in DMF (Figure S15).

Excitation Energy Attenuation by Water. In addition to the energy transfer between nanoparticles and water molecules, we believe that the absorption of water, particularly near 980 nm, which can attenuate the excitation light, also plays a critical role in the quenching of upconversion emission. Figure 6a and Figure S16 show the absorption of DMF solvent containing varied water content. At very low concentration, water absorption at ~980 nm is almost negligible (Figure S16). An obvious absorption at ~980 nm was observed when the water content was ~1 vol %, and the absorption was almost linearly correlated to the water content. Similar absorption behaviors were also observed while measuring both DMSO and ethanol solvents with varied water content (Figures S17 and S18). We therefore reason that water absorption is partially responsible for the upconversion emission quenching at high water concentration (typically >1 vol %).

To prove the influence of direct excitation energy absorption by water molecules, we designed a noncontact water content detection in organic solvent (Figure 6b). In this design, upconversion nanoparticles dispersed in cyclohexane are sealed in a quartz cuvette and the cuvette is then aligned with the other cuvette containing testing sample. Upon 980 nm laser excitation, the light passes through the testing sample to pump upconversion nanoparticles. Owing to the absorption of excitation light by water molecules in the testing sample, upconversion emission of the nanoparticles is reduced, indicating the presence of water. As a proof-of-concept experiment, we probed the water content, ranging from 0 to 100 vol %, in DMF. A sequential luminescence decrease was observed with the increase of water content (Figures 6c and 6d). Apart from DMF, we can also probe the water content in other organic solvents, like DMSO and ethanol, by using this noncontact method (Figures S19 and S20). These findings suggest that water molecule absorption at 980 nm partially contributes to the upconversion emission quenching during water probing. Moreover, the results also demonstrate another facile method for water sensing by using upconversion nanoparticles as indicators.

On a separate note, water induced upconversion luminescence quenching is caused by a variety of quenching effects, including energy transfer and direct water absorption of excitation energy. Further in-depth understanding of the quenching effect should facilitate new applications of upconversion nanomaterials.

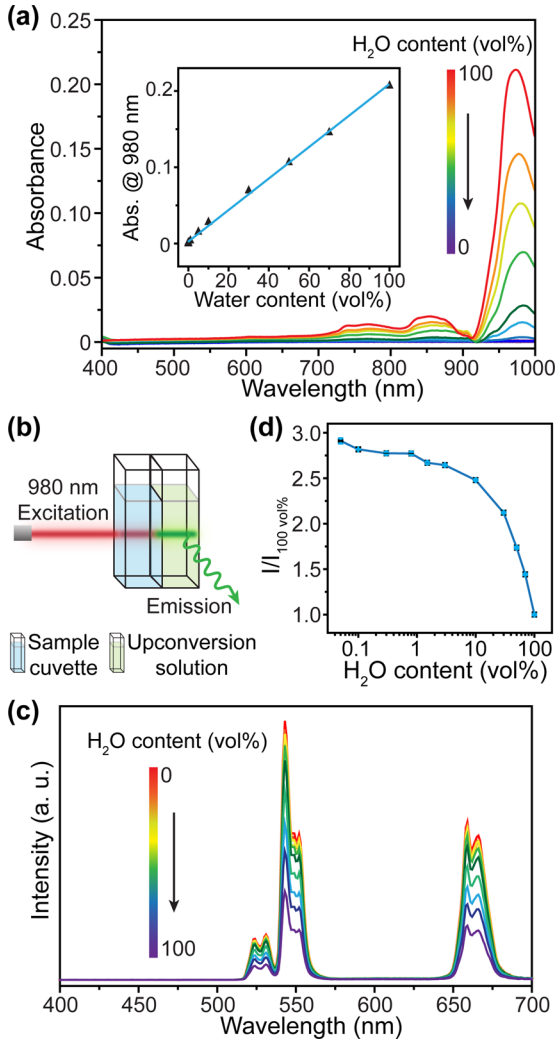

Figure 6. (a) Absorption spectra of DMF containing varied water content (0−100 vol %). The corresponding absorption at 980 nm as a function of water content is shown as inset. (b) Schematic illustration of the noncontact water content detection in organic solvent using upconversion nanoparticles. (c) Upconversion emission changes of $NaYF_4$:Yb/Er nanoparticles as a function of H_2O concentration (0−100 vol %) in DMF utilizing noncontact method. (d) Corresponding relative emission intensity ($I/I_{100\,vol\%}$) dependence on H_2O concentration (0.05−100 vol %) as illustrated in (c). Note that the emission intensity was obtained by integrating the emission from 400 to 700 nm, and the line serves as a guide to the eye. Data are presented as the average from three measurements.

CONCLUSIONS

We have demonstrated a facile water sensing by using upconversion nanoparticles, with the assistance of nonlinear upconversion process. The water molecules can suppress the nanoparticle emission through both energy transfer and excitation energy depletion. Utilizing the efficient water induced upconversion quenching, we have achieved a detection down to 80 ppm water in DMF in the presence of ligand-free nanoparticles. Moreover, we also have shown that water probing can be realized through a noncontact detection method. Benefiting from photostable upconversion emission, our design can be used for long-term and real-time monitoring

DOI: 10.1021/acsami.5b10192
ACS Appl. Mater. Interfaces 2016, 8, 847−853

of water content in challenging conditions. In addition, beyond water sensing in polar solvents demonstrated here, further modification of the upconversion nanoparticles can make these nanoprobes suitable for different conditions, such as in nonpolar solvent, gas phase, and biological environment. We believe that these findings should provide new insights into the design of upconversion nanoparticles based optical sensors.

■ ASSOCIATED CONTENT

Supporting Information

The Supporting Information is available free of charge on the ACS Publications website at DOI: 10.1021/acsami.5b10192.

XRD patterns, FTIR, microscopy images, absorption spectra, additional upconversion emission spectra (Figures S1−S20) and decay curve analyses (Tables S1−S2) (PDF)

■ AUTHOR INFORMATION

Corresponding Authors

*X.X.: e-mail, iamxjxie@njtech.edu.cn.
*L.H.: e-mail, iamlhuang@njtech.edu.cn.
*W.H.: e-mail, iamwhuang@njtech.edu.cn

Notes

The authors declare no competing financial interest.

■ ACKNOWLEDGMENTS

This work was supported by National Natural Science Foundation of China (Grant 21401103), National Basic Research Program of China (973 Program, Grant 2015CB932200), Natural Science Foundation of Jiangsu Province (Grants BM2012010, BE2015699), and Synergetic Innovation Center for Organic Electronics and Information Displays. We thank Dr. X. Liu, Dr. Y. Wang, and Q. Sun for decay curve measurement, and we thank Dr. Q. Su and Dr. X. Li for their suggestions.

■ REFERENCES

(1) Lee, W.; Jin, Y.; Park, L.; Kwak, G. Fluorescent Actuator Based on Microporous Conjugated Polymer with Intramolecular Stack Structure. *Adv. Mater.* **2012**, *24*, 5604−5609.

(2) Douvali, A.; Tsipis, A. C.; Eliseeva, S. V.; Petoud, S.; Papaefstathiou, G. S.; Malliakas, C. D.; Papadas, I.; Armatas, G. S.; Margiolaki, I.; Kanatzidis, M. G.; Lazarides, T.; Manos, M. J. Turn-On Luminescence Sensing and Real-Time Detection of Traces of Water in Organic Solvents by a Flexible Metal-Organic Framework. *Angew. Chem.* **2015**, *127*, 1671−1676.

(3) Wang, L.; Li, Y. Luminescent Coordination Compound Nanospheres for Water Determination. *Small* **2007**, *3*, 1218−1221.

(4) Yao, M.; Chen, W. Hypersensitive Luminescence of Eu^{3+} in Dimethyl Sulfoxide as a New Probing for Water Measurement. *Anal. Chem.* **2011**, *83*, 1879−1882.

(5) Kreno, L. E.; Leong, K.; Farha, O. K.; Allendorf, M.; Van Duyne, R. P.; Hupp, J. T. Metal-Organic Framework Materials as Chemical Sensors. *Chem. Rev.* **2012**, *112*, 1105−1125.

(6) Deng, Q.; Li, Y.; Wu, J.; Liu, Y.; Fang, G.; Wang, S.; Zhang, Y. Highly Sensitive Fluorescent Sensing for Water based on Poly(m-aminobenzoic acid). *Chem. Commun.* **2012**, *48*, 3009−3011.

(7) Suzuki, N.; Fukazawa, A.; Nagura, K.; Saito, S.; Kitoh-Nishioka, H.; Yokogawa, D.; Irle, S.; Yamaguchi, S. A Strap Strategy for Construction of an Excited-State Intramolecular Proton Transfer (ESIPT) System with Dual Fluorescence. *Angew. Chem., Int. Ed.* **2014**, *53*, 8231−8235.

(8) Liu, D.; Lu, K.; Poon, C.; Lin, W. Metal-Organic Frameworks as Sensory Materials and Imaging Agents. *Inorg. Chem.* **2014**, *53*, 1916−1924.

(9) Qin, P.; Han, C.; Huang, D. A Fluorescent Probe for Water Content in Ethanol based on a Complex of Ruthenium(II). *Anal. Methods* **2014**, *6*, 202−206.

(10) Gao, F.; Luo, F.; Chen, X.; Yao, W.; Yin, J.; Yao, Z.; Wang, L. Fluorometric Determination of Water in Organic Solvents using Europium Ion-Based Luminescent Nanospheres. *Microchim. Acta* **2009**, *166*, 163−167.

(11) Cheng, S.; Chau, L. Colloidal Gold-Modified Optical Fiber for Chemical and Biochemical Sensing. *Anal. Chem.* **2003**, *75*, 16−21.

(12) Lin, P.; Giammarco, J.; Borodinov, N.; Savchak, M.; Singh, V.; Kimerling, L. C.; Tan, D. T. H.; Richardson, K. A.; Luzinov, I.; Agarwal, A. Label-Free Water Sensors Using Hybrid Polymer-Dielectric Mid-Infrared Optical Waveguides. *ACS Appl. Mater. Interfaces* **2015**, *7*, 11189−11194.

(13) Liang, Y. Y. Automation of Karl Fischer Water Titration by Flow Injection Sampling. *Anal. Chem.* **1990**, *62*, 2504−2506.

(14) Dong, H.; Du, S.; Zheng, X.; Lyu, G.; Sun, L.; Li, L.; Zhang, P.; Zhang, C.; Yan, C. Lanthanide Nanoparticles: From Design toward Bioimaging and Therapy. *Chem. Rev.* **2015**, *115*, 10725−10815.

(15) Chen, G.; Qiu, H.; Prasad, P. N.; Chen, X. Upconversion Nanoparticles: Design, Nanochemistry, and Applications in Theranostics. *Chem. Rev.* **2014**, *114*, 5161−5214.

(16) Han, S.; Deng, R.; Xie, X.; Liu, X. Enhancing Luminescence in Lanthanide-Doped Upconversion Nanoparticles. *Angew. Chem., Int. Ed.* **2014**, *53*, 11702−11715.

(17) Li, L.; Wu, P.; Hwang, K.; Lu, Y. An Exceptionally Simple Strategy for DNA-Functionalized Up-Conversion Nanoparticles as Biocompatible Agents for Nanoassembly, DNA Delivery, and Imaging. *J. Am. Chem. Soc.* **2013**, *135*, 2411−2414.

(18) Feng, W.; Han, C.; Li, F. Upconversion-Nanophospor-Based Functional Nanocomposites. *Adv. Mater.* **2013**, *25*, 5287−5303.

(19) Gai, S.; Li, C.; Yang, P.; Lin, J. Recent Progress in Rare Earth Micor/Nanocrystals: Soft Chemical Synthesis, Luminescent Properties, and Biomedical Applications. *Chem. Rev.* **2014**, *114*, 2343−2389.

(20) Li, X.; Zhang, F.; Zhao, D. Lab on Upconversion Nanoparticles: Optical Properties and Applications Engineering via Designed Nanostructure. *Chem. Soc. Rev.* **2015**, *44*, 1346−1378.

(21) Chen, Z.; Zhou, L.; Bing, W.; Zhang, Z.; Li, Z.; Ren, J.; Qu, X. Light Controlled Reversible Inversion of Nanophosphor-Stabilized Pickering Emulsions for Biphasic Enantioselective Biocatalysis. *J. Am. Chem. Soc.* **2014**, *136*, 7498−7504.

(22) Wong, H.; Tsang, M.; Chan, C.; Wong, K.; Fei, B.; Hao, J. *In vitro* Cell Imaging using Multifunctional Small Sized $KGdF_4$:Yb^{3+},Er^{3+} Upconverting Nanoparticles Synthesized by a One-Pot Solvothermal Process. *Nanoscale* **2013**, *5*, 3465−3473.

(23) Fan, W.; Shen, B.; Bu, W.; Chen, F.; Zhao, K.; Zhang, S.; Zhou, L.; Peng, W.; Xiao, Q.; Xing, H.; Liu, J.; Ni, D.; He, Q.; Shi, J. Rattle-Structured Multifunctional Nanotheranostics for Synergetic Chemo-/Radiotherapy and Simultaneous Magnetic/Luminescent Dual-Mode Imaging. *J. Am. Chem. Soc.* **2013**, *135*, 6494−6503.

(24) Cheng, L.; Yang, K.; Li, Y.; Chen, J.; Wang, C.; Shao, M.; Lee, S.; Liu, Z. Facile Preparation of Multifunctional Upconversion Nanoprobes for Multimodal Imaging and Dual-Targeted Photothermal Therapy. *Angew. Chem.* **2011**, *123*, 7523−7528.

(25) Huang, P.; Zheng, W.; Zhou, S.; Tu, D.; Chen, Z.; Zhu, H.; Li, R.; Ma, E.; Huang, M.; Chen, X. Lanthanide-Doped $LiLuF_4$ Upconversion Nanoprobes for the Detection of Disease Biomarkers. *Angew. Chem., Int. Ed.* **2014**, *53*, 1252−1257.

(26) Lu, Y.; Zhao, J.; Zhang, R.; Liu, Y.; Liu, D.; Goldys, E. M.; Yang, X.; Peng, X.; Sunna, A.; Lu, J.; Shi, Y.; Leif, R. C.; Huo, Y.; Shen, J.; Piper, J. A.; Robinson, J. P.; Jin, D. Tunable Lifetime Multiplexing using Luminescent Nanocrystals. *Nat. Photonics* **2014**, *8*, 32−36.

(27) Sedlmeier, A.; Gorris, H. H. Surface Modification and Characterization of Photon-Upconverting Nanoparticles for Bioanalytical Applications. *Chem. Soc. Rev.* **2015**, *44*, 1526−1560.

DOI: 10.1021/acsami.5b10192
ACS Appl. Mater. Interfaces 2016, 8, 847−853

(28) Zhou, S.; Zheng, W.; Chen, Z.; Tu, D.; Liu, Y.; Ma, E.; Li, R.; Zhu, H.; Huang, M.; Chen, X. Dissolution-Enhanced Luminescent Bioassay Based on Inorganic Lanthanide Nanoparticles. *Angew. Chem.* **2014**, *126*, 12706−12710.
(29) Li, Z.; Liang, T.; Lv, S.; Zhuang, Q.; Liu, Z. A Rationally Designed Upconversion Nanoprobe for in Vivo Detection of Hydroxyl Radical. *J. Am. Chem. Soc.* **2015**, *137*, 11179−11185.
(30) Wang, J.; Wei, T.; Li, X.; Zhang, B.; Wang, J.; Huang, C.; Yuan, Q. Near-Infrared-Light-Mediated Imaging of Latent Fingerprints based on Molecular Recognition. *Angew. Chem., Int. Ed.* **2014**, *53*, 1616−1620.
(31) Li, C.; Liu, J.; Alonso, S.; Li, F.; Zhang, Y. Upconversion Nanoparticles for Sensitive and In-depth Detection of Cu^{2+} ions. *Nanoscale* **2012**, *4*, 6065−6071.
(32) Wang, F.; Wang, J.; Liu, X. Direct Evidence of a Surface Quenching Effect on Size-Dependent Luminescence of Upconversion Nanoparticles. *Angew. Chem., Int. Ed.* **2010**, *49*, 7456−7460.
(33) Arppe, R.; Hyppänen, I.; Perälä, N.; Peltomaa, R.; Kaiser, M.; Würth, C.; Christ, S.; Resch-Genger, U.; Schäferling, M.; Soukka, T. Quenching of the Upconversion Luminescence of $NaYF_4$:Yb^{3+},Er^{3+} and $NaYF_4$:Yb^{3+},Tm^{3+} Nanophosphors by Water: the Role of the Sensitizer Yb^{3+} in Non-Radiative Relaxation. *Nanoscale* **2015**, *7*, 11746−11757.
(34) Chen, D.; Liu, L.; Huang, P.; Ding, M.; Zhong, J.; Ji, Z. Nd^{3+}-Sensitized Ho^{3+} Single-Band Red Upconversion Luminescence in Core-Shell Nanoarchitecture. *J. Phys. Chem. Lett.* **2015**, *6*, 2833−2840.
(35) Wang, J.; Deng, R.; MacDonald, M. A.; Chen, B.; Yuan, J.; Wang, F.; Chi, D.; Hor, T. S. A.; Zhang, P.; Liu, G.; Han, Y.; Liu, X. Enhancing Multiphoton Upconversion through Energy Clustering at Sublattice Level. *Nat. Mater.* **2014**, *13*, 157−162.
(36) Johnson, N. J. J.; van Veggel, F. C. J. M. Sodium Lanthanide Fluoride Core-Shell Nanocrystals: A General Perspective on Epitaxial Shell Growth. *Nano Res.* **2013**, *6*, 547−561.
(37) Haase, M.; Schäfer, H. Upconverting Nanoparticles. *Angew. Chem., Int. Ed.* **2011**, *50*, 5808−5829.
(38) Li, Z.; Zhang, Y.; Jiang, S. Multicolor Core/Shell-Structured Upconversion Fluorescent Nanoparticles. *Adv. Mater.* **2008**, *20*, 4765−4769.
(39) Chen, B.; Peng, D.; Chen, X.; Qiao, X.; Fan, X.; Wang, F. Establishing the Structural Integrity of Core-Shell Nanoparticles against Elemental Migration using Luminescent Lanthanide Probes. *Angew. Chem., Int. Ed.* **2015**, *54*, 12788−12790.
(40) Shen, J.; Chen, G. Y.; Vu, A.; Fan, W.; Bilsel, O. S.; Chang, C.; Han, G. Engineering the Upconversion Nanoparticle Excitation Wavelength: Cascade Sensitization of Tri-doped Upconversion Colloidal Nanoparticles at 800 nm. *Adv. Opt. Mater.* **2013**, *1*, 644−650.
(41) Zhong, Y.; Tian, G.; Gu, Z.; Yang, Y.; Gu, L.; Zhao, Y.; Ma, Y.; Yao, J. Elimination of Photon Quenching by a Transition Layer to Fabricate a Quenching-Shield Sandwich Structure for 800 nm Excited Upconversion Luminescence of Nd^{3+}-Sensitized Nanoparticles. *Adv. Mater.* **2014**, *26*, 2831−2837.
(42) Xie, X.; Gao, N.; Deng, R.; Sun, Q.; Xu, Q.; Liu, X. Mechanistic Investigation of Photon Upconversion in Nd^{3+}-Sensitized Core-Shell Nanoparticles. *J. Am. Chem. Soc.* **2013**, *135*, 12608−12611.
(43) Chan, E. M.; Han, G.; Goldberg, J. D.; Gargas, D. J.; Ostrowski, A. D.; Schuck, P. J.; Cohen, B. E.; Milliron, D. J. Combinatorial Discovery of Lanthanide-Doped Nanocrystals with Spectrally Pure Upconverted Emission. *Nano Lett.* **2012**, *12*, 3839−3845.
(44) Dong, H.; Sun, L.; Wang, Y.; Ke, J.; Si, R.; Xiao, J.; Lyu, G.; Shi, S.; Yan, C. Efficient Tailoring of Upconversion Selectivity by Engineering Local Structure of Lanthanides in Na_xREF_{3+x} Nanocrystals. *J. Am. Chem. Soc.* **2015**, *137*, 6569−6576.
(45) Liu, X.; Kong, X.; Zhang, Y.; Tu, L.; Wang, Y.; Zeng, Q.; Li, C.; Shi, Z.; Zhang, H. Breakthrough in Concentration Quenching threshold of Upconversion Luminescence *via* Spatial Separation of the Emitter Doping Area for Bio-applications. *Chem. Commun.* **2011**, *47*, 11957−11959.
(46) Saboktakin, M.; Ye, X.; Oh, S. J.; Hong, S.; Fafarman, A. T.; Chettiar, U. K.; Engheta, N.; Murray, C. B.; Kagan, C. R. Metal-Enhanced Upconversion Luminescence Tunable through Metal Nanoparticle−Nanophosphor Separation. *ACS Nano* **2012**, *6*, 8758−8766.
(47) Wang, Y.; Song, S.; Liu, J.; Liu, D.; Zhang, H. ZnO-Functionalized Upconverting Nanotheranostic Agent: Multi-Modality Imaging-Guided Chemotherapy with On-Demand Drug Release Triggered by pH. *Angew. Chem., Int. Ed.* **2015**, *54*, 536−540.
(48) Chen, P.; Jia, H.; Zhang, J.; Han, J.; Liu, X.; Qiu, J. Magnetic Tuning of Optical Hysteresis Behavior in Lanthanide-Doped Nanoparticles. *J. Phys. Chem. C* **2015**, *119*, 5583−5588.
(49) Wang, F.; Liu, X. Recent Advances in the Chemistry of Lanthanide-Doped Upconversion Nanocrystals. *Chem. Soc. Rev.* **2009**, *38*, 976−989.
(50) Bogdan, N.; Vetrone, F.; Ozin, G. A.; Capobianco, J. A. Synthesis of Ligand-Free Colloidally Stable Water Dispersible Brightly Luminescent Lanthanide-Doped Upconverting Nanoparticles. *Nano Lett.* **2011**, *11*, 835−840.

DOI: 10.1021/acsami.5b10192
ACS Appl. Mater. Interfaces 2016, 8, 847−853